Eur. Phys. J. B **23**, 521–531 (2001)

THE EUROPEAN PHYSICAL JOURNAL B

EDP Sciences

Static magneto-polarizability of cylindrical nanostructures

S. Pleutin[a] and A. Ovchinnikov

Max-Planck-Institut für Physik Komplexer Systeme, Nöthnitzer Straße 38, 01187 Dresden, Germany

Received 29 March 2001 and Received in final form 8 August 2001

Abstract. The static polarizability of cylindrical systems is shown to have a strong dependence on a uniform magnetic field applied parallel to the tube axis. This dependence is demonstrated by performing exact numerical diagonalizations of simple cylinders (rolled square lattices), armchair and zig-zag carbon nanotubes (rolled honeycomb lattices) for different electron-fillings. At low temperature, the polarizability as function of the magnetic field has a discontinuous character where plateau-like region are separated by sudden jumps or peaks. A one to one correspondence is pointed out between each discontinuity of the polarizability and the magnetic-field induced cross-over between the ground state and the first excited state. Our results suggest the possibility to use measurements of the static polarizability under magnetic field to get important informations about excited states of cylindrical systems such as carbon nanotubes.

PACS. 77.22.-d Dielectric properties of solids and liquids – 78.40.Ri Fullerenes and related materials – 75.20.-g Diamagnetism, paramagnetism, and superparamagnetism – 73.23.-b Electronic transport in mesoscopic systems

1 Introduction

Cylindrical like systems, as nanotubes of carbon or one dimensional stacks of ring organic molecules, show, in the absence of time-reverse symmetry breaking perturbations, two energetically degenerated families of one-electron states. One is for electrons moving in clockwise direction, the other is for electrons moving in counter-clockwise direction. A magnetic field applied along the cylindrical axis breaks time-reverse symmetry. The degeneracies are then lifted and a diamagnetic current is induced. If one considers the behaviour of the energies of the many-particle states, one finds lot of level crossing induced by the magnetic field. In other words, accidental degeneracies are created at some values of the external magnetic field. This means also that the ground state changes when the magnetic field varies.

Very recently [1] the study of the polarisability of cylindrical systems under magnetic field was suggested as a possible probe to analyse their electronic structures. The underlying mechanism of this proposed new spectroscopy is quite simple. The magnetic field induces level crossings as already mentioned. As a consequence of that, changes of the ground state occur which at some fields is degenerate. Applying in addition an electric field, two kinds of effect are expected near those magnetic-field-induced accidental degeneracies: (i) at the crossing points, a linear Stark effect may occur if there exists a non vanishing matrix element of the perturbation between the two crossing states, resulting in divergencies in the polarisability, (ii) when the matrix element between these two states is vanishing, the system shows a quadratic Stark effect but the difference between the quadratic Stark coefficients of the two states involved creates discontinuities in the response function. A careful analysis of the linear electric susceptibility should then provide important informations about properties of excited states such as their energies and symmetries. A few years ago it was already pointing out that a magnetic field should have pronounced effects on the polarisability but for quite different materials and purposes, *i.e.* in [2–4] small metallic particles (rings, disks or spheres) were considered in connection with weak localization. In particular, it was found that the polarizability should be greater in magnetic field than in zero field because of the disappearance of weak localization. This theoretical prediction was observed very recently in the ac polarizability of mesoscopic rings [5].

Square lattices and honeycomb lattices (nanotubes) rolled-up into cylinders with uniform electric and magnetic fields both applied along the cylindrical axis were studied in [1]. With this configuration full quantum calculations were not possible for large systems. Instead, since the electric field creates a smoothly varying potential across the cylinder, a semi-classical expression for the dielectric function was used. With this approximate approach, the discontinuities of the polarisability were well observed – resulting in extraordinary rich structures – however, the effects of possible linear Stark effect were not described.

The main purpose of this work is to establish and extent on the basis of full quantum calculations the ideas

[a] e-mail: pleutin@physik.uni-freiburg.de

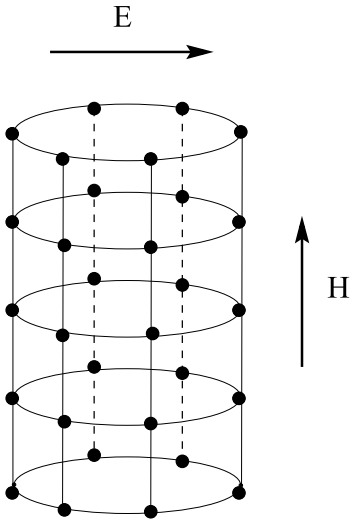

Fig. 1. Cylinder made of rolled square lattice placed in two uniform fields: an electric-field, E, perpendicular to the cylindrical axis and a magnetic field, H, parallel to it. The same field configuration is adopted for carbon nanotubes (rolled honeycomb lattices).

and concepts discussed in [1] using semi-classical calculations. For that purpose, the very same cylindrical systems are considered, *i.e.* square and honeycomb lattices, but with the modification that the electric field is applied perpendicularly to the cylindrical axis (*cf.* Fig. 1). The net advantage of this choice is to allow for a separation of variable, *i.e.* the two degrees of freedom corresponding to the motion of the electrons along the circumference and the cylindrical axis of the cylinder can be treated separately. The exact calculation of the polarisability (*i.e.* by fully quantum treatment) is then possible even for very large systems. The first conclusions of [1] are confirmed and the appearance of linear Stark effect are well identified. Additionally, the effects of the shape of a system and of the Zeeman interaction on the dielectric function are discussed as well as differences occurring in the magnetic field dependent spectrum of armchair and zig-zag nanotubes. Finally perturbative calculations of the dielectric response are done. They are in perfect agreement with the exact results as long as we remain in the linear regime.

Before proceeding further we want to stress that all the necessary conditions are available nowadays to realize the experiments we are proposing. On one hand very accurate measurements of the polarisability at very low temperatures are possible [5,6]. A spectacular example was given by the recent observations of a strong magnetic-field dependence of the polarisability of multicomponent glasses in the mK regime [6]. On the other hand, systems with diameters in the mesoscopic range are required in order to realize the experiment; however large circumference nanotubes are routinely produce today [7] and could be first candidates of interest.

2 Rolled square lattices

We consider first cylinders in form of rolled square lattices. As already mentioned in the introduction, two uniform fields are applied to those systems: a magnetic field H, parallel to the cylindrical axis, and an electric field E, perpendicular to it (*cf.* Fig. 1). In this work we are concerned only with orbital magnetism. Therefore we will neglect the spin of the electrons. The dynamic of the spinless fermions are described in terms of the following standard tight-binding model.

$$\begin{aligned}\hat{H} = & t\sum_{n,m}(a^{\dagger}_{n+1,m}a_{n,m}\mathrm{e}^{\mathrm{i}\frac{2\pi}{N}\phi} + \text{h.c.}) \\ & + t_p\sum_{n,m}(a^{\dagger}_{n,m+1}a_{n,m} + \text{h.c.}) \\ & + v\sum_{n,m}\cos(\frac{2\pi}{N}n)a^{\dagger}_{n,m}a_{n,m}. \end{aligned} \quad (1)$$

Different sites are labelled by the indices n along the circumference running from 1 to N, and m along the cylindrical axis running from 1 to M. The total number of sites of the cylinder is thus given by NM. $a^{\dagger}_{n,m}$ ($a_{n,m}$) is the creation (annihilation) operator of a spinless electron on site (n,m). t and t_p are the nearest-neighbour hopping integrals, ϕ is the magnetic flux in unit of the elementary flux $\phi_0 = \frac{\hbar c}{e}$ and v denotes the potential related to the electric field, *i.e.* $v = eRE$, with R being the radius of the cylinder.

The field E is supposed to be small enough so that we are in the linear response regime. The magnetic flux is proportional to the magnetic field and the section area of the cylinder

$$\phi = \frac{N^2a^2H}{8\pi^2} \quad (2)$$

where a is the lattice constant on the circumference. We are interested in systems of a mesoscopic size along the circumference. Typically, R should be in the range of several tens of nanometres. Then the corresponding flux quantum is of order several tens of tesla which is nowadays reachable experimentally.

The effects of the Zeeman interaction are not considered in this work. With this interaction, if one includes also the spin-orbital coupling, changes can arise in the calculated polarizability especially at high magnetic field or low electronic density as briefly discussed below. The effects of the orbital magnetism discussed in this work are expected to be in any case predominant. Nevertheless, for practical purpose, the effects of the Zeeman and spin-orbital interactions should be also incorporated.

Moreover the electron-electron interaction terms are not explicitely introduced in this work. Instead they are supposed to be included in the effective one-electron parameters of our model in the spirit of the Fermi-liquid theory of Landau. An explicit treatment of these interactions which lead to screening of the electric field could produce important qualitative changes especially in the strong coupling limit as it was shown for ring systems [8].

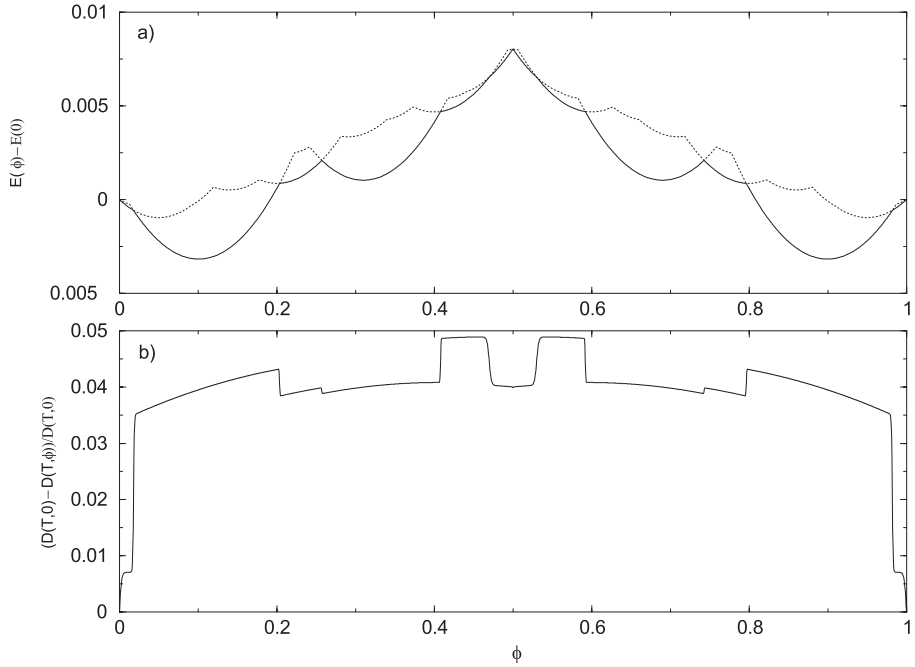

Fig. 2. Cylinder with $N = 101$, $M = 100$ and $N_e = 100$, the numbers of site along the circumference, along the cylindrical axis and number of electrons (respectively). (a) Energies of the ground state (full line) and of the first excited state (dotted line) as function of the magnetic flux, ϕ, without electric field (the references are the energies without magnetic field). (b) Polarizability $(D(T,0) - D(T,\phi))/D(T,0)$, at $k_BT = 10^{-5}t$ and for $v = eER = 10^{-3}t$ as function of the magnetic flux; t is the hopping integral defined in (1), E the electric field and R the radius of the cylinder.

Without electric field, *i.e.* for $v = 0$, the spectrum of (1) is given by

$$\epsilon_{p,q} = 2t\cos(\frac{2\pi}{N}(p+\phi)) + 2t_p\cos(\frac{\pi}{M+1}q) \qquad (3)$$

with $-N/2 \leq p \leq N/2-1$ and $1 \leq q \leq M$. We have applied open boundary conditions at the ends of the cylinder. It has to be associated with the one-electron wave functions

$$|\Psi_{p,q}\rangle = \sqrt{\frac{2}{N(M+1)}}\sum_{n=1}^{N}\sum_{m=1}^{M} e^{i\frac{2\pi}{N}pn} \times \sin(\frac{\pi}{M+1}qm)a^\dagger_{n,m}|0\rangle \qquad (4)$$

where $|0\rangle$ is the vacuum.

At zero magnetic field, *i.e.* for $\phi = 0$, the spectrum is two fold degenerate, $\epsilon_{p,q} = \epsilon_{-p,q}$, except for the states with $p = 0$ and $p = -N/2$. Adopting the convention that states with positive p are for electrons running in clockwise direction then states with negative p describe electrons moving in counterclockwise direction.

A finite magnetic field ($\phi \neq 0$), breaks time-reversal symmetry and implies lifting the two-fold degeneracy and inducing a diamagnetic current. As a consequence, the energy spacings of the many-electron states are continuously changing with increasing magnetic field. This is shown in Figure 2a for the lowest eigenstates.

For a finite electric field ($v \neq 0$), it is not possible anymore to solve analytically model Hamiltonian (1). However, for the configuration shown in Figure 1, we can treat separately the variables n and m. This reduces the study to a one dimensional Hamiltonian for a ring in an applied electric field

$$\hat{H}_R = t\sum_n (a^\dagger_{n+1}a_n e^{i\frac{2\pi}{N}\phi} + \text{h.c.}) + v\sum_n \cos(\frac{2\pi}{N}n)a^\dagger_n a_n. \qquad (5)$$

This is Harper's model which has been extensively used in very different contexts of condensed matter physics and which can be treated. It should be noticed that, this model, *i.e.*, a ring placed in an uniform electric field – is similar to a rectangular lattice with hopping integrals given by t and $v/2$ and threaded by a magnetic field with a flux given by $\phi = \frac{2\pi}{N}$.

In the following, we shall assume that $t = t_p$. The relative value of these two transfer integrals has considerable influences on the dielectric function but we leave this study to future considerations.

Once the spectrum is known, we calculate the induced dipole moment D, as function of the magnetic field and temperature T as follows.

$$D(T,\phi) = \frac{\text{Tr}\hat{d}e^{-\beta(\hat{H}-\mu)}}{\text{Tr}e^{-\beta(\hat{H}-\mu)}} \qquad (6)$$

where, as usual, $\beta = \frac{1}{k_BT}$ and $\hat{d}$ is the dipole operator

$$\hat{d} = eR\sum_{n,m}\cos(\frac{2\pi}{N}n)a^\dagger_{n,m}a_{n,m}. \qquad (7)$$

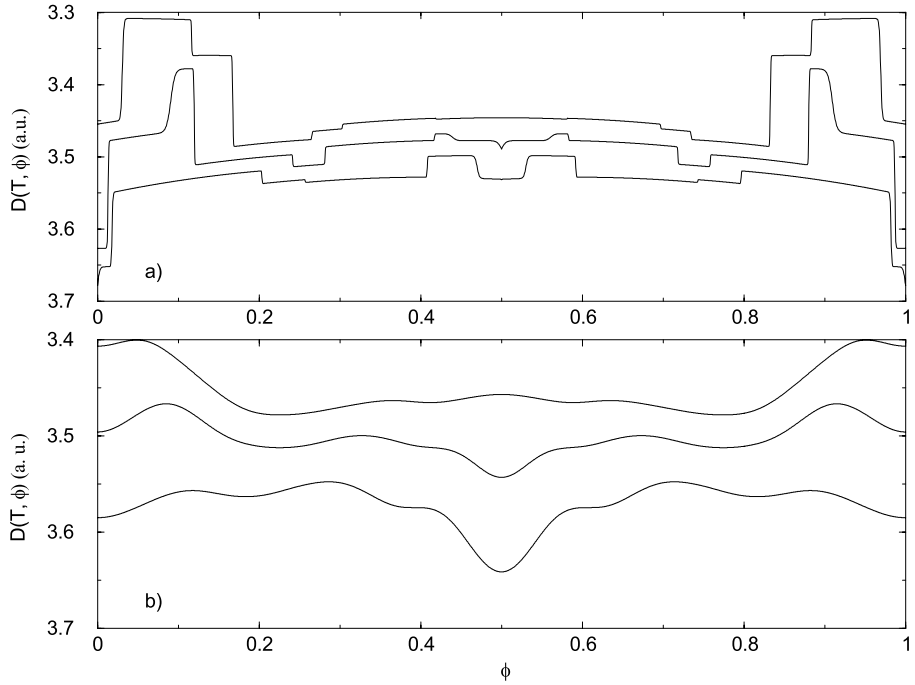

Fig. 3. Polarizability of a cylinder with $N = 101$ and $M = 100$ as function of the magnetic flux ϕ in arbitrary units (a.u.). (a) For $N_e = 100, 101, 102$ from the bottom to the top at a temperature of $k_B T \simeq 10^{-1}$ K. (b) The same but for $k_B T \simeq 10$ K.

We show in Figure 2b the magnetic field dependence of the polarisability for a cylinder with $N = 101$ and $M = 100$ and a very few electrons on it, $N_e = 100$ (which corresponds to a band filling of only 1%). In this example, the electric field is such that $v = 10^{-3}t$ and the temperature is $k_B T = 10^{-5}t$. We choose this example because it shows very clearly the main behaviours of the dielectric response. In particular we choose $N = 101$ because this gives an illustration of the signature of the linear Stark effect.

First of all the induced dipole moment as function of the magnetic field is periodic with a period of ϕ_0 and is symmetric with respect to $\phi_0/2$; these symmetries are already apparent in the spectrum (3). Second, the induced dipole moment shows clearly two main characteristics: (i) we can notice the presence of small peaks at $\phi = 0, 1/2, 1$, (ii) the induced dipole moment is a discontinuous function showing several jumps separating plateau-like sections. Note that there is a slight curvature in the whole spectrum, which is related to the persistent current induced by the magnetic field.

As noticed before, a magnetic field induces crossing between the energies of the ground state and the first excited state (Fig. 2a). As it can be seen in Figures 2, there is a one to one correspondence between level crossing at zero electric field and each kink in the induced dipole moment.

At each crossing, the ground state of the system changes. These two states which are crossing respond differently to an applied electric field. Both produce a quadratic Stark effect but generally of different size. This explains why the induced dipole moment is not a continuous function of the magnetic field.

Near the crossing points, the response of the system will depend on whether or not there is a nonzero matrix element of the electric field between the two states involved. If the matrix element vanishes, the picture described above is valid. On the contrary, if there is interaction between those states, due to the degeneracy, the response will become a linear (instead of quadratic) Stark effect resulting in peaks of the induced dipole moment. More precisely, using the expression of the wave function (4), the matrix elements of the dipole operator can be calculated

$$\langle \Psi_{p,q} | \hat{d} | \Psi_{p',q'} \rangle = eR\delta_{p',p\pm1}\delta_{q',q}. \tag{8}$$

With this equation, it is easy to see that linear Stark effect could occur only for the following very particular values of the magnetic flux: $\phi = 0, 1/2, 1$. These are precisely the values for which one gets peaks in our first example (Fig. 2b).

It is worth notice that large enough Coulomb interaction could change drastically the selection rules (8). Appearance of linear Stark effects for new values of the magnetic flux could then give a way to quantify importance of electronic correlation effects.

At low enough temperature, one deals essentially with the spectroscopy of a few levels around the Fermi level. Therefore it is not surprising that the induced dipole moment for a well definite system, *i.e.*, one which is well ordered, well oriented and of well defined size (N, M), depends strongly on the electronic density. This is clearly apparent from Figures 3a and b. They are for the very same system than before but for three different electron fillings $N_e = 100, 101$ and 102. At such a low density,

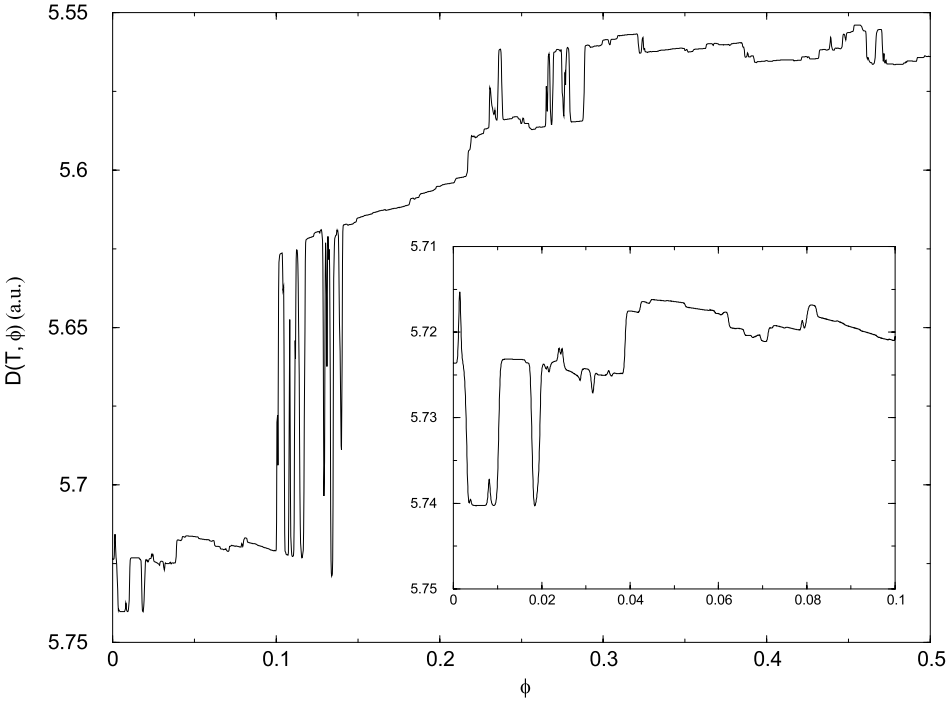

Fig. 4. Polarizability of a cylinder with $N = 101$, $M = 1000$ and $N_e = 20\,000$ as function of the magnetic flux at $k_B T = 10^{-5} t$ in arbitrary units (a.u.). In the inset: zoom of the small magnetic field part.

the relevant mean level spacing behaves as $\Delta E \approx 1/N^2$. Figure 3a is for a temperature lower than ΔE by one order of magnitude while Figure 3b is for a temperature higher than ΔE by one order of magnitude. With a typical value for t ($t \approx 2$ eV) one can estimate a temperature of 10^{-1} K for the spectrum 3a and 10 K for the spectrum 3b. With these figures we want to emphasize the unique sensitivity of the proposed measurements and its corollary which is the necessity to work at very small temperature in order to get the maximum informations.

In Figure 4, we show again the induced dipole moment for the same electric field and temperature but for a bigger cylinder, $N = 101$ and $M = 1000$, and more electrons on it, $N_e = 20\,000$ (electron density of 20%). The response appears to be much more complex but shows the same characteristics of peaks and plateau-like parts separated by discontinuous jumps. This is more apparent in the inset which shows a zoom of the spectrum at low magnetic fields.

Today it is possible to measure accurately very small variations in the real part of the dielectric function [6]. Therefore, the dramatic magnetic field effects on the static polarisability of mesoscopic cylindrical systems, discussed in this work, could be measured and analysed. Several important informations about excited states could then be obtained. First, the positions of the discontinuities and peaks should give informations about the energies of the excited states. The nature of the response – linear or quadratic Stark effect could be detected and therefore should give information about the symmetry of the excited states. The magnitude of the response should give also informations about the coupling constants. Finally, the different curvatures observed in the whole spectrum could give information related to the persistent current induced by the magnetic field.

Of course, as it was already mentioned, the model we are studied gives an oversimplified view of the reality. In order to go to realistic systems several other aspects remain to be clarified. The very important case of electron-electron interactions will be the subjects of subsequent works. In the following, we discuss briefly, first, possible influences of the shape of the cylindrical cross-section and, second, the role plays by Zeeman interaction. For practical purposes, it is certainly necessary to study in details both of these points.

Influences of the shape. Case of elliptical cross-section. Until now, we have considered only cylindrical systems with circular cross-section. With this particular shape, a uniform electric field creates the cosine potential appearing in (1). The electronic eigenstates of these cylindrical systems are characterized by a pair of wave vectors, k and q, for the motion along the circumference and the cylindrical axis respectively. The cosine potential of equation (1) couples states of different wave vectors, k_1, q_1 and k_2, q_2, in such a way that the following selection rules are fulfilled $\Delta k = k_1 - k_2 = \pm\frac{2\pi}{N}$ and $\Delta q = q_1 - q_2 = 0$, as already discussed above. However, there exist many cases where the section of the cylinder may have different shapes. One could think, for instance, of a one dimensional stack of large organic polycyclic molecules which do not form regular circles according to the well known hybridisation properties of carbon atom. With different shapes the cosine potential will be affected undergoing new selection rules. These new selection rules could in turns influence

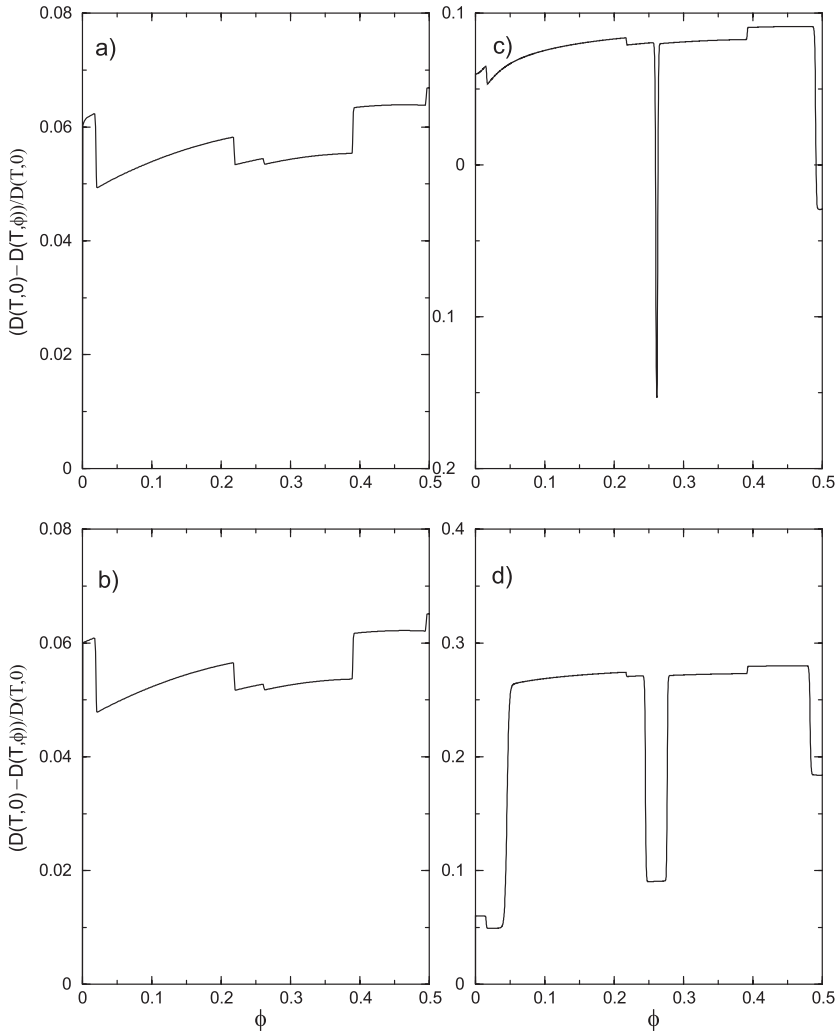

Fig. 5. Polarizability $(D(T,0)-D(T,\phi))/D(T,0)$ of an ellipse and a cylinder with $N = 100$, $M = 100$ and $N_e = 100$ as function of the magnetic flux, ϕ, at $k_BT = 10^{-5}t$. (a) Ellipse with $\frac{a^2}{b^2} = 0.25$ and $v = 10^{-3}t$. (b) Cylinder with $v = 10^{-3}t$. (c) Ellipse with $\frac{a^2}{b^2} = 0.25$ and $v = 10^{-2}t$. (d) Cylinder with $v = 10^{-2}t$.

substantially the induced dipole moment. For illustration we consider here the case of an elliptical cross-section and compare its response with the one of a circular section.

For a general cross-section the dipole operator takes the following form

$$\hat{d} = e\sum_{n,m} R(n)\cos(\Theta(n))a^{\dagger}_{n,m}a_{n,m} \qquad (9)$$

where $R(n)$ is the distance of the site n to the cylindrical axis and $\Theta(n)$ the corresponding polar angle with respect to some arbitrary axis. The sites are supposed to be equally space. $R(n)$ and $\Theta(n)$ are determined under this condition. The model (1) is then still valid and the electronic spectrum of the system without electric field is still given by equation (3).

An ellipse is characterized by two parameters, the major axis $2a$, and the minor axis $2b$. We give an example for an elliptical cylinder with $N = 100$, $M = 100$, $N_e = 100$ and $b/a = 0.5$.

In Figures 5a and b are reported the induced dipole moment for elliptical and circular systems with $v = 10^{-3}t$; Figures 5c and d present the same results but for $v = 10^{-2}t$.

For an ellipse, there is additional coupling between k states which do not fulfilled the original selection rules $\Delta k = \pm\frac{2\pi}{N}$ and $\Delta q = 0$. At small electric fields (linear regime) these additional couplings yield very smooth changes only on the shape of the induced dipole moment; as can be seen in Figures 5a and b, only the amplitudes are slightly modified. However, at higher electric fields more dramatic changes appear (Figs. 5c and d). This is the case in our example where one can notice, for instance, the appearance of a new peak at $\phi \simeq 0.26$ for an elliptical section.

Influences of the Zeeman interaction. For realistic consideration of fermions with spin 1/2, the Zeeman interaction combined with the spin-orbital interaction must be

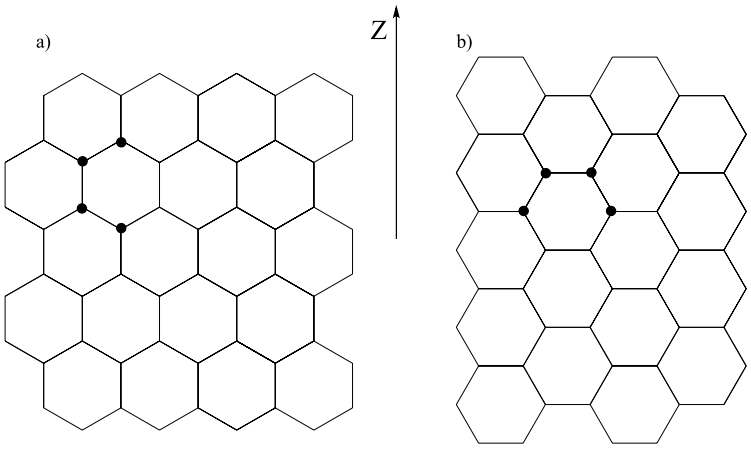

Fig. 6. Carbon nanotubes are rolled honeycomb lattices around the Z-axis. Here are represented part of the honeycomb lattice for (a) zig-zag carbon-nanotubes and (b) armchair carbon-nanotubes. They are both achiral nanotubes, similar to cylindrical systems with 4 carbon atoms per unit cell marked here by the black dots.

clarified. In this subsection we give only a first hint in that direction.

The Zeeman Hamiltonian is given by

$$\hat{H}_Z = g\mu_{\rm B}\mathbf{SB} \tag{10}$$

where $\mathbf{S}$ is the total spin of the system, $\mu_{\rm B}$, the Bohr magneton and g, the Landé factor. Due to the effect of this interaction every one-particle level will be split into a spin-up and spin-down component by a term proportional to ϕ/N^2. Therefore, by considering also the effects of the spin-orbit coupling, the whole spectrum could be changed: both, the positions of the accidental degeneracies (discontinuities) could be shifted and the intensities of the induced dipole moment could be modified. The importance of those changes can be estimated by considering the ratio of the Zeeman energy ϕ/N^2 and, $\Delta(n)$, the level spacing of the one-dimensional ring Hamiltonian (5)

$$\begin{aligned}\Delta(n) &= 4t\sin(\frac{2\pi}{N})\sin(\frac{2\pi}{N}(n+\phi+\frac{1}{2})) \\ &\simeq \frac{4\pi}{N}\sin(\frac{2\pi}{N}n).\end{aligned} \tag{11}$$

The spacing is not an uniform function of N. It behaves as $1/N^2$ at the bottom of the band, and as $1/N$ in the middle of the band. With this consideration one may conclude that the Zeeman plus spin-orbit coupling can become important in the case of (i) high magnetic fields or/and (ii) low electronic density.

3 Armchair and zig-zag carbon nanotubes

Within the class of cylindrical materials, carbon nanotubes are certainly among the most interesting and fascinating. They are honeycomb lattices rolled into cylinders [9]. Part of their interests comes from their unique interplay between geometry and electronic properties [7]. Indeed, a single-wall nanotube can be either metallic or semiconducting depending on its diameter and its chirality. This fact was recognized very soon after their discovery using tight binding models [10] and from first principle calculations [11].

We consider in the following the two simplest kinds of nanotube: the so-called zig-zag nanotubes (Fig. 6a), which are semiconductors (conductors) if the number of unit cell N is not (is) a multiple of 3, and the armchair nanotubes (Fig. 6b), which are always metallic [7]. They are the two kinds of nanotube having the highest symmetry. Moreover they are the only two examples showing no chirality. Because of this last characteristics, they can be considered as a kind of rolled square lattice but with four carbon atoms per unit cell; these units are shown on the Figures 6 for both systems. In the presence of an uniform magnetic field along the cylindrical axis, the spectrum is formally similar for the two systems

$$\epsilon_{p,q} = \pm(1 + u_p \pm (u_p v_q)^{1/2})^{1/2} \tag{12}$$

where for zig-zag nanotubes

$$\begin{aligned} u_p &= 2(1+\cos(\tfrac{2\pi}{N}(p+\phi))), \quad \text{with} \quad p = 1,..,N \\ v_q &= 2(1+\cos(\tfrac{\pi}{M+1}q)), \quad \text{with} \quad q = 1,..,M \end{aligned} \tag{13}$$

and for armchair nanotubes

$$\begin{aligned} u_p &= 2(1+\cos(\tfrac{\pi}{M+1}p)), \quad \text{with} \quad p = 1,..,M \\ v_q &= 2(1+\cos(\tfrac{2\pi}{N}(q+\phi))), \quad \text{with} \quad q = 1,..,N. \end{aligned} \tag{14}$$

The roles of u_p and v_q are just exchanged from one case to the other. For calculating these spectra we have used the transformation from a hexagonal lattice to rectangular lattice with four sites per unit-cell introduced in [12].

With an electric field, the spectrum can no longer be obtained analytically however – as for the case of rolled square lattices – since the systems chosen have no chirality, it is still possible to treat separately the variables

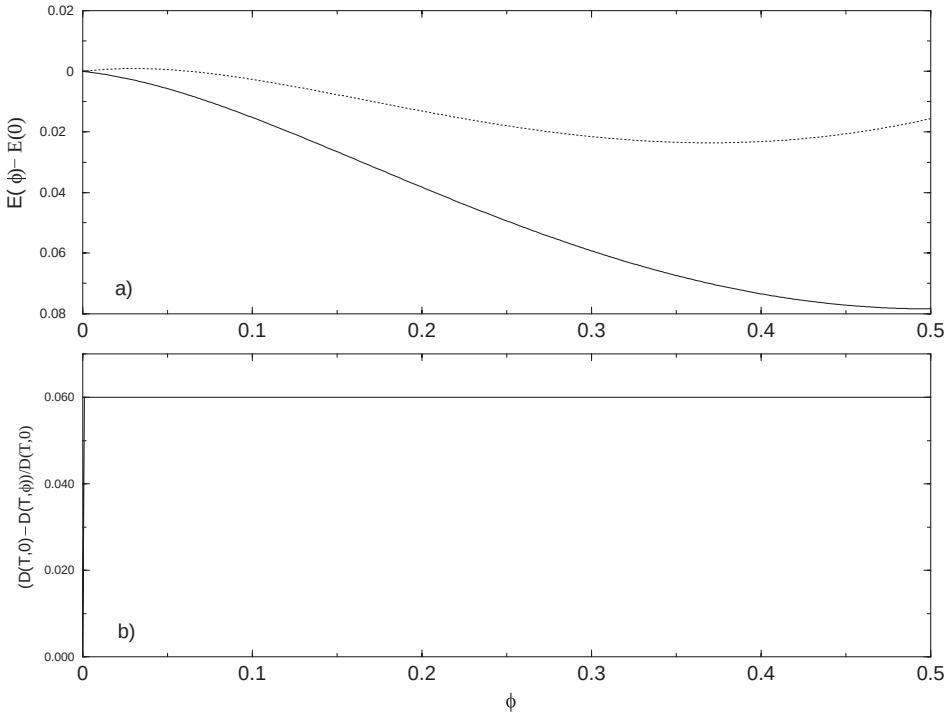

Fig. 7. Armchair nanotube with $N = 50$, $M = 500$ and $N_e = 50\,000$ (half-filling) at $k_BT = 10^{-5}t$. (a) Energies of the ground and first excited state as function of the magnetic flux ϕ (the references are the energies without magnetic field). (b) Polarizability $(D(T,0) - D(T,\phi))/D(T,0)$ for $v = 10^{-3}t$ as function of the magnetic flux.

along the circumference and the cylindrical axis. The effective systems we have then to consider explicitely are rings of N units, containing each four carbon atoms, but where the coupling constants depend on the wave vector in the cylindrical direction. Proceeding that way, it is then possible to study exactly the response to an electric field even for very large systems.

In our calculations we neglect the two ends of the nanotubes which consist of a "hemisphere" of a fullrene [7]. Since the scale along the cylindrical axis is in our calculations much larger than the one along the diameter this approximation should be justified (in reality ratio as large as 10^5 between these two characteristic scales are usual).

We present first, results for armchair and zig-zag nanotubes with $N = 50$ and $M = 500$ at half-filling, $N_e = 50\,000$, for a small electric field, $v = 10^{-3}t$, and low temperature, $k_BT = 10^{-5}t$. For this choice of N, the zig-zag nanotube is semiconductor. The Figures 7a and b show the ground state and first excited state energies and the induced dipole moment, respectively, as function of the magnetic flux for the armchair nanotube; the Figures 8a and b show the same results but for the zig-zag nanotube.

The electronic structure of carbon nanotubes under uniform magnetic field parallel to the tube axis was already study in the past using kp perturbation theory [13] and exact calculations [14]. A magnetic field induced metal-insulator transition was then predicted: a semiconductor nanotube becomes metallic for high enough magnetic field and, reversely, a metallic nanotube becomes semiconductor. This dramatic behaviour predicted theoretically could be an explanation for magnetoresistance experiments on carbon nanotube bundles [15] and more recent ones on multi-wall carbon nanotubes [16].

We recover these results in our calculations. The magnetic field opens a gap in the case of the armchair nanotube (Fig. 7a); on the contrary, the magnetic field tends to close the gap for the zig-zag nanotube until $\phi \simeq 0.35$ where the gap starts to increase smoothly (Fig. 8a). These different behaviours are also apparent in the polarizability as can be seen on the Figures 7b and 8b; the response functions follow the evolution of the band gaps in both cases. Additionally, one can notice the peak observed at $\phi = 0$ for the armchair nanotube showing that the ground state and the first excited states are directly coupled *via* the electric-field given rise to a strong linear Stark effect.

The static electric polarizability tensor (without magnetic field) of carbon nanotubes, $\boldsymbol{\alpha}$, was studied in the past for the half-filled case, using a tight-binding model [17]. It was shown that the α_{zz} component of the polarizability tensor is proportional to R/E_g^2, where E_g is the band gap and R is the radius of the tube, while α_{xx} is independent of E_g and is proportional to R^2. In our case we are concerned with α_{xx} and we have check the above mentioned scaling law for zig-zag and armchair nanotubes. Our results, for these particular achiral examples, are consistent with the study in [17].

The α_{zz} component was studied in [1] with an applied magnetic field but using a semi-classical approximation which do not allow us to do direct comparison with the results of the present work. However, it is reasonable to

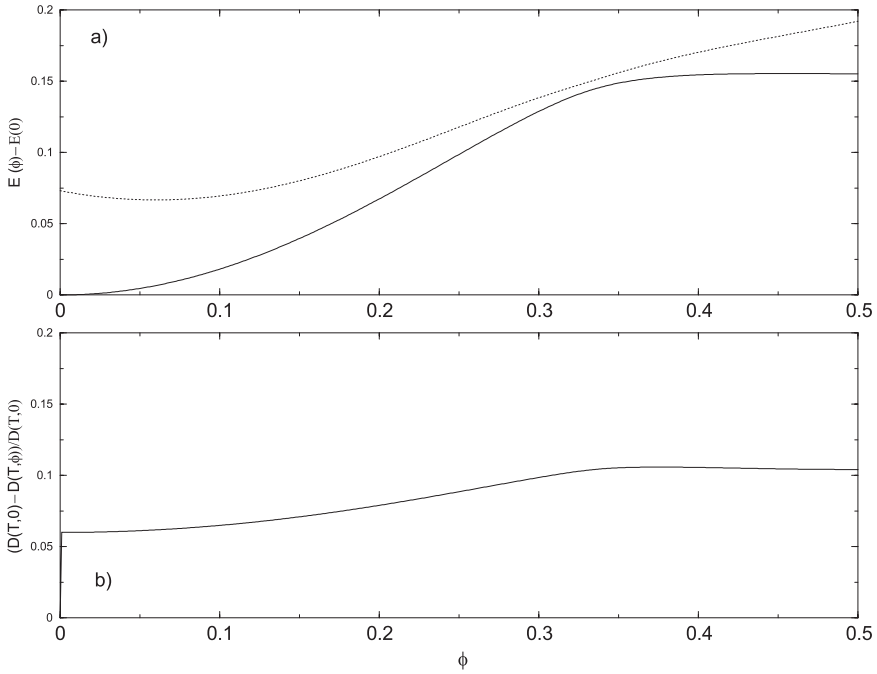

Fig. 8. Zig-zag nanotube with $N = 50$, $M = 500$ and $N_e = 50\,000$ (half-filling) at $k_BT = 10^{-5}t$. (a) Energies of the ground and first excited state as function of the magnetic flux ϕ (the references are the energies without magnetic field). (b) Polarizability $(D(T,0) - D(T,\phi))/D(T,0)$ for $v = 10^{-3}t$ as function of the magnetic flux ϕ.

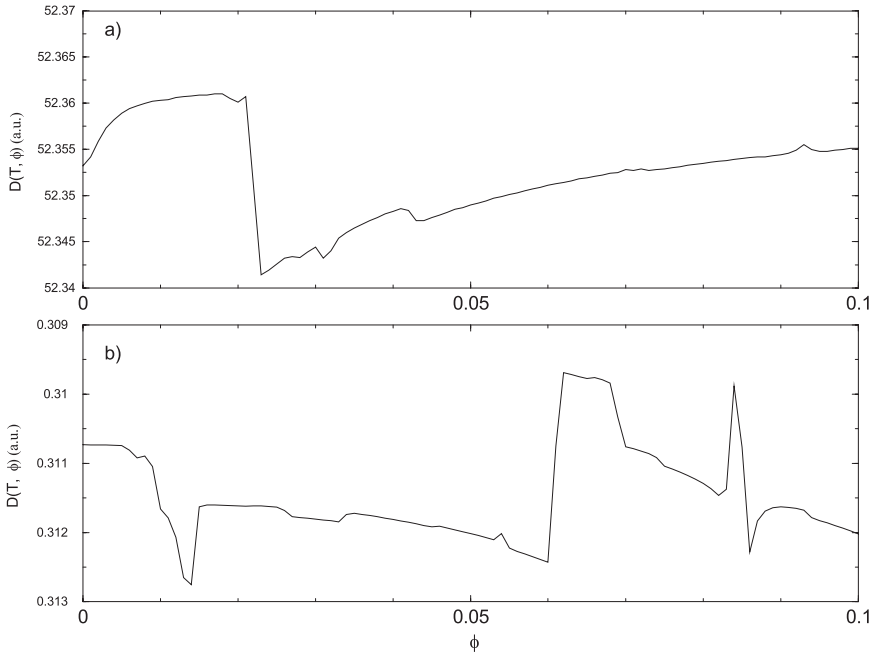

Fig. 9. Polarizability in arbitrary units (a.u.) of (a) armchair and (b) zig-zag nanotubes with $N = 50$, $M = 500$, $N_e = 49\,000$, $k_BT = 10^{-5}t$ and $v = 10^{-3}t$ as function of the magnetic flux ϕ.

think the absolute values of the polarizability tensor will not change drastically by applying a magnetic field. Therefore, according to the results of [17], one can conclude that the static-magneto polarizability should be much more intense for longitudinal electric field than transversal electric field.

The second results we want to show, as an illustration, are for the two very same systems but slightly away from half-filling ($N_e = 49\,000$). The corresponding induced dipole moment are shown in Figures 9a and b, for armchair and zig-zag nanotubes, respectively, at low magnetic field only. Without going into any details one immediately sees that both responses are considerably much intricate than the ones at half-filling, indicating more complicated behaviours of the ground and first-excited states as function of the magnetic field. The analysis of such responses

should give important informations about the electronic spectrum of these compounds.

4 Perturbative results

In the linear regime, where we mainly worked, a perturbative expression for the induced dipole moment should be appropriate. Let us consider a system described by the general Hamiltonian $\hat{H} = \hat{H}_0 + \hat{V}$ where $\hat{H}_0$ is for the system without electric field and $\hat{V}$ takes into account the effect of the electric field acting as a perturbation. At second order in perturbation theory, the induced dipole moment is given by

$$D(T,\phi) = \frac{1}{2}\sum_{I,J} \frac{|\langle \Psi_I|\hat{V}|\Psi_J\rangle|^2}{\epsilon_I - \epsilon_J} f_{\rm F}(\epsilon_{\rm I})(1 - f_{\rm F}(\epsilon_J)) \quad (15)$$

where $\hat{H}_0|\Psi_{\rm I}\rangle = \epsilon_{\rm I}|\Psi_{\rm I}\rangle$ and $f_{\rm F}(\epsilon) = 1/(\mathrm{e}^{\beta(\epsilon-\mu)}+1)$ is the Fermi distribution function, μ being the chemical potential.

Let us illustrate the effectiveness of these perturbative calculations for the particular case of the cylinders of the Section 2, where the selection rules are particularly restrictive. Indeed, in this case $\hat{V}$ is given by the dipolar operator (7) and the wave function, $|\Psi_I\rangle$, by Bloch functions (4), $|\Psi_{p,q}\rangle$. The matrix elements of the dipole operator are then given by the equation (8), resulting in a simple expression for the polarizability of a cylinder

$$D(T,\phi) = \frac{e^2R^2}{2M}\sum_{p=0}^{N-1}\sum_{q=1}^{M} f_{\rm F}(\epsilon_{p,q}) \times \left\{ \frac{1 - f_{\rm F}(\epsilon_{p-1,q})}{\epsilon_p(\phi) - \epsilon_{p-1}(\phi)} + \frac{1 - f_{\rm F}(\epsilon_{p+1,q})}{\epsilon_p(\phi) - \epsilon_{p+1}(\phi)} \right\} \quad (16)$$

where we add the dependence over the magnetic flux ϕ. R is the radius of the cylinder, M and N the number of sites along the cylindrical axis and along the circumference, respectively, $\epsilon_{p,q}$ the spectrum defined in (3) and $\epsilon_p(\phi) = 2t\cos(\frac{2\pi}{N}(p+\phi))$.

We have compared this perturbative expression with exact calculations for different cylinders and several choices of temperature and values for the hopping integrals, t and t_p. The results are always in perfect accordance, except for the very particular points where linear Stark effect occur, as far as we remain in the linear regime. In this regime all the curves presented in this work could have been obtained by the perturbative expression (16). This could give a simplified framework to perform in the future more sophisticated analysis of the problem like inclusion of electron-electron interaction, for instance.

For nanotubes, more complex expressions will result due to less restrictive selection rules. However, such perturbative calculations can also be done.

5 Conclusions

The main purpose of this work was to demonstrate, using exact calculations, the strong magnetic field dependence of the static polarizability of cylindrical systems when the magnetic field is parallel to the tube axis. This was already predicted in [1] on the basis of semi-classical analysis.

The demonstration was done for two kinds of system. On one hand we have considered rolled square lattices and, on the other hand, two kinds of non-chiral carbon nanotubes, *i.e.*, metallic armchair nanotubes and the zigzag nanotubes, which can be either semiconducting or metallic [7]. For all these cases, the polarizability was shown to present very complex structures as function of the magnetic field in which one can identify two different characteristics (*cf.* Fig. 2): (i) the polarizability is a non-continuous function with sudden jumps separating plateau-like regions (ii) additionally, small peaks may appear for special values of the magnetic field in place of jumps.

A full understanding of these complicated behaviours was given by following the behaviour of the ground state by increasing the magnetic field: due to the Aharonov-Bohm effect, many changes of ground state occurs and for some values of the magnetic field accidental degeneracies happen where the ground state becomes two fold degenerate. A one to one correspondence is found between the accidents in the polarizability and the accidental degeneracies of the ground state. Each plateau-like region of the polarizability corresponds to a quadratic Stark effect with a coefficient proper to the corresponding magnetic-field induced ground state. Each peak corresponds to a linear Stark effect appearing at accidental degeneracies when there is direct coupling between the two states involved (*cf.* Fig. 2). Therefore, it seems possible to study the static polarizability under magnetic field in view to obtain informations about excited states of cylindrical systems.

For ring shape cylinders and with a one-electron picture, the peaks due to linear Stark effect appear for very particular magnetic field values, $\phi = 0, 1/2, 1$. The situation could be very different for different shape – as we have seen for elliptical tubes – or with Coulomb interaction.

All the results shown in this work are for selected cylindrical systems. Indeed, since the proposed measurements are extremely sensitive to the characteristic sizes of the systems, N and M, and to the electron density, it is necessary to be able to select with high accuracy an individual system. However, it is already possible to perform measurements on individual single-wall nanotube [18], for instance, which make us to believe that the proposed experiments are nowaday possible to realize.

Finally, we have done our studies with a one electron picture but the screening due to electron-electron interaction is very important and can diminish considerably the absolute value of $D(T,0)$ [17]. However, it is reasonable to believe that the screening effects should be independent of the applied magnetic field. Therefore, the ratio $\frac{D(T,\phi)-D(T,0)}{D(T,0)}$ should remain unchanged with screening effects.

Several extensions of this work are necessary. For the near future we are planning to work in three directions. (i) We plan to consider instead of individual, a set of

cylindrical systems – with a particular attention for set of nanotubes and multi-wall carbon nanotubes. (ii) An explicit treatment of the electron-electron interaction is absolutely needed especially since important qualitative changes could occur for ring systems [8] and very important effects were shown on transport measurements of single-wall nanotubes [19]. (iii) Disorder effects (topological or substitutional disorder) are also of importance for the properties we are interested in [20] and should be considered in the future.

It is a pleasure for us to thank Prof. P. Fulde for his support and careful reading of the manuscript.

References

1. P. Fulde, A.A. Ovchinnikov, Eur. Phys. J. B **17**, 623 (2000).
2. K.B. Efetov, Phys. Rev. Lett. **76**, 1908 (1996).
3. Y. Noat, B. Reulet, H. Bouchiat, Europhys. Lett. **36**, 701 (1996).
4. Ya. M. Blanter, A.D. Mirlin, Phys. Rev. B **57**, 4566 (1998).
5. R. Deblock, Y. Noat, H. Bouchiat, B. Reulet, D. Mailly, Phys. Rev. Lett. **84**, 5379 (2000).
6. P. Strehlow, C. Enss, S. Hunklinger, Phys. Rev. Lett. **80**, 5361 (1998); P. Strehlow, M. Wohlfahrt, A.G.M. Jansen, R. Haueisen, G. Weiss, C. Ens, S. Hunklinger, Phys. Rev. Lett. **84**, 1938 (2000).
7. R. Saito, G. Dresselhaus, M.S. Dresselhaus, *Physical Properties of Carbon Nanotubes* (Imperial College Press, 1998).
8. F.V. Kusmartsev, J. Phys. Cond. Matt. **3**, 3199 (1991); for a review see A.A. Zvyagin, I.V. Krive, Low Temp. Phys. **21**, 533 (1995).
9. S. Iijima, Nature **354**, 56 (1991); S. Iijima, T. Ishihashi, Nature **363**, 603 (1993).
10. R. Saito, M. Fujita, G. Dresselhaus, M.S. Dresselhaus, Appl. Phys. Lett. **60**, 2204 (1992); N. Hamada, S. Sawada, A. Oshiyama, Phys. Rev. Lett. **68**, 1579 (1992).
11. J.W. Mintmire, B.I. Dunlap, C.T. White, Phys. Rev. Lett. **68**, 631 (1992).
12. K. Wakabayashi, M. Fujita, H. Ajiki, M. Sigrist, Phys. Rev. B **59** 8271 (1999).
13. H. Ajiki, T. Ando, J. Phys. Soc. Jpn. **62**, 2470 (1993).
14. J.P. Lu, Phys. Rev. Lett. **74**, 1123 (1995).
15. S.N. Song, X.K. Wang, R.P.H. Chang, J.B. Ketterson, Phys. Rev. Lett. **72**, 697 (1994).
16. A. Fujiwara, K. Tomiyama, H. Suematsu, M. Yumura, K. Uchida, Phys. Rev. B **60**, 13492 (1999).
17. L.X. Benedict, S.G. Louie, M.L. Cohen, Phys. Rev. **52**, 8541 (1995).
18. S.J. Tans, M.H. Devoret, H. Dai, A. Thess, R.E. Smalley, L.J. Geerligs, C. Dekker, Nature **386**, 474 (1997).
19. S.J. Tans, M.H. Devoret, R.J.A. Groeneveld, C. Dekker, Nature **394**, 761 (1998); Y. Oreg, K. Byczuk, B.I. Halperin, Phys. Rev. Lett. **85**, 365 (2000).
20. S. Roche, G. Dresselhaus, M.S. Dresselhaus, R. Saito, Phys. Rev. B **62**, 16092 (2000).